

# Partial Discharge Evolution under Half-sine Voltage Excitation

G. Fu, H. Edin, G. D. P. Mahidhar & P. Janus

*School of Electrical Engineering, Royal Institute of Technology, Stockholm, Sweden*

## Abstract

Partial discharges (PD) analysis is the common technique for detection and identification of dielectric defects. Certain PD characteristics can be an early sign of degradation. For further understanding, combined voltages can enhance the analysis of PD characteristics in some specific cases. This paper presents an experimental study on the PD appearance under repetitive negative half-sine voltage excitation, as such a combination of AC and DC voltage. Adopting the time-resolved PD pattern technique, PD signals originated from dielectric barrier corona discharge (DBCD) source are recorded in time domain by a DL750 Scope Corder. Preliminary filtered results indicated the strong relationship between surface charge accumulation and back discharge, a time delay movement of back discharge can be clearly observed on the pattern during ‘relaxation time period’ with various insulation materials.

## 1. Introduction

Partial discharge detection methods have been extensively researched as the evolution tools of insulation condition. The corona discharge is one of the most typical discharge types, which happens in partial position in gas with enough electric field. Surface charge accumulation will take effect while insulation material falls in between of the electrodes, DBCD can happen along with different PD phenomena [1]-[2].

The enhancement of experimental methods allows more precise analysis on some specific discharge conditions and abnormal PD phenomena [1]. Recently, combined voltages have been frequently used in PD measurements [3]-[14]. For example, a sinusoidal AC voltage superimposed on DC voltage [3] was applied to partial discharge qualification in HVDC system, which was called ‘Direct Current Periodic (DCP)’. By the use of square and semi-square voltages, the relation between PD extinction voltage and voltage rise time [4]-[6], transition of PD magnitude with aging [7], PD behavior of material with void [8], were targeted studied. The utilization of combined voltages is aimed at obtaining clearer and extra PD information at different discharge conditions. For instance, unipolar half-sine waveform with pause time interval [9] was applied to explore an enhanced PD diagnostic method, which clarified the influence of charge accumulation on PD behavior. A triangular voltage [10]-[11] was used to study the PD activity based on the method called ‘Pulse-Sequence Analysis (PSA)’, which can analyze PD pattern under time domain. As for PD pattern recognition, sawtooth

[12], trapezoidal [13] and square waveforms were used to improve the distinction on surface and cavity discharge. In [14], an exponential decay voltage was utilized to reveal the great influence of  $dV/dt$  on PD behavior. Combined and editable waveform, especially unipolar voltage, could simulate the space charge accumulation condition in DC voltage, but also generate ‘phase’ information with its AC component, which provides the possibility on the PD pattern analysis.

In DC and unipolar condition, space charge accumulation effect should be taken into consideration. Ionic wind is a gas flow phenomenon originating from corona discharge [15], where ions in drift region move in the electric field direction, transmitting their momentum to molecules in the air gap and generating the wind, which will change the space charge distribution on the surface of insulation material [16]-[18].

In this paper, a unipolar negative half-sine voltage was utilized for studying the influence of charge accumulation on an insulating surface. A relaxation phase with variable duration was introduced and its influence on the PD behavior was investigated. The initial measurements showed a PD anomaly under the time-resolved DBCD PD test, as shown in Figure 1. This behavior was further experimentally investigated. Five different materials were tested to investigate this phenomenon. A possible explanation through the ‘ionic wind’ theory is discussed.

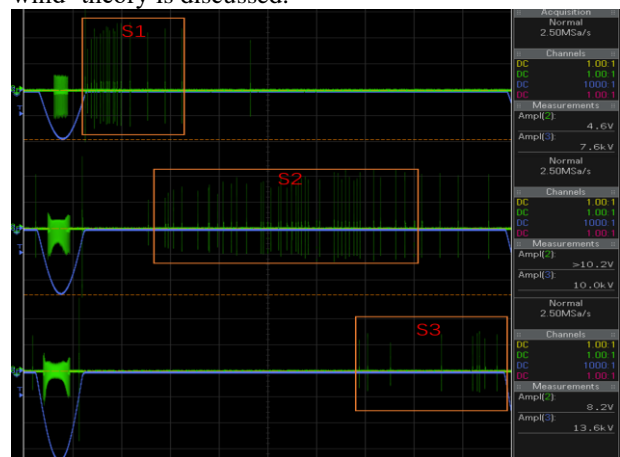


**Figure 1. Oscilloscope image of corona discharges during the negative half-sine voltage and the observed back discharge movement at increasing applied peak voltage.**

## 2. Experimental method

To study the influence of charge accumulation and the influence of charge decay during a zero-voltage ‘relaxation’ phase, unipolar half-sine voltage was found

to give an interesting behavior and applied to the DBCD sample cell, based on the time-resolved partial discharge measurement system.

### 2.1. PD measurement system

The partial discharge measurement system consisted of a HP 33120A function generator, a TREK 20/20 C high voltage amplifier, a PMK PPE 20 kV high voltage probe(1000:1), a Yokogawa DL750 Scope Corder, a coupling capacitor, a detection impedance with a resistance of  $39 \Omega$  in parallel with  $1.65 \text{ nF}$  capacitor and a personal computer, as shown in Figure 2.

The half-sine voltage waveform was edited in MATLAB, transmitted to and generated by the function generator, then amplified 2000 times through the TREK amplifier. The voltage was submitted to the dielectric barrier needle-plane electrode system and caused partial discharges at a sufficiently high voltage magnitude. The PD pulse current went through the detection impedance and transformed to voltage signal, then recorded by the Scope Corder. The Scope Corder works as an oscilloscope with 12 bits A/D resolution, 10 MSa/s sampling rate, and a 250 MSa deep memory, which allows long time recording.

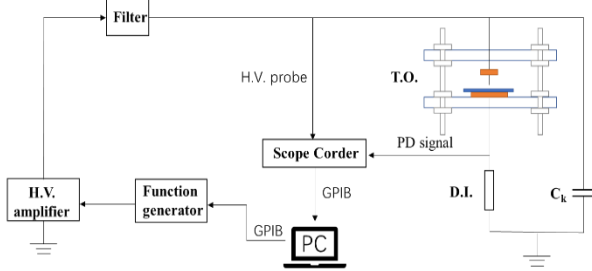


Figure 2. Diagram of PD measurement system

### 2.2. Half-sine voltage waveform

The voltage used in this paper is a negative unipolar half-sine waveform, as shown in Figure 3, which is comprised of two parts: a unipolar half of sinusoidal waveform and a relaxation time period.

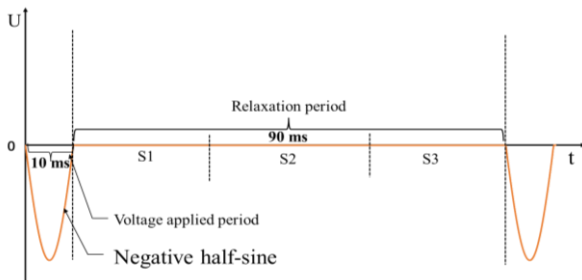


Figure 3. Negative half-sine waveform

In this study, the first part of the applied voltage is the negative half-period of a 50 Hz sinusoidal waveform with time length of 10 ms. The second part is the relaxation time period with 0 V voltage level, providing, in these experiments, a 90 ms time interval for the movement and distribution of the surface charges. During this period, back discharges will take place because of the space charges accumulated on the surface of insulation. For further trend analysis, the relaxation time period was divided into three stages (S1, S2, S3) to indicate the time-of-occurrence of back discharges, and its dependence on voltage levels was investigated based on the preliminary results.

### 2.3. Sample cell and insulation materials

All the partial discharges were generated in the typical needle-plane dielectric barrier corona setup of which the sample cell is shown in Figure 4.

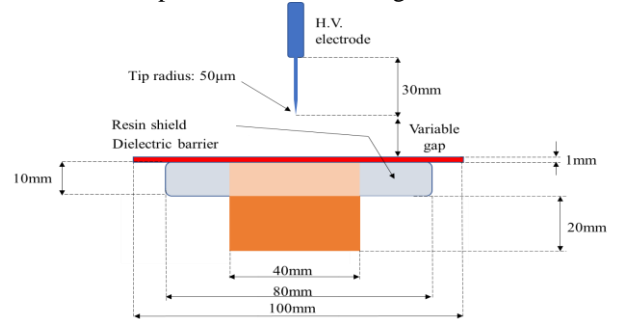


Figure 4. Sample cell of corona discharge

The ground electrode is a conductive brass cylinder casted in an epoxy resin. The brass cylinder has a diameter of 40 mm and thickness of 30 mm, the resin shield has a diameter of 80 mm and thickness of 10 mm. An insulation plate with 100 mm diameter and 1 mm thickness was placed on the ground electrode, keeping the air gap distance as 10 mm. A needle electrode with the length of 30 mm and the tip radius  $15 \mu\text{m}$  was used as high voltage electrode, which was fixed on the sample platform by a brass holder with a banana socket. The needle tip was aligned to the center of insulation plate.

Five different materials were used: polytetrafluoroethylene (PTFE), polyethylene (PE), polycarbonate (PC), polyvinylchloride (PVC), and unimpregnated pressboard. All the materials were cut to the same geometry, and the physical properties of the materials are shown in the Table 1, where the bulk resistivity and surface resistivity were calculated based on the stable value of current and voltage, which were measured by KEITHLEY 6105 resistivity adapter and KEITHLEY 6514 electrometer at 400 V.

Table 1. Bulk and surface resistivity measured at 400 V

	PTFE	PE	PC	PVC	Pressboard
Basic properties	nature, soft	nature, PE1000	transparent, rigid	nature, rigid	dry
PDIV / kV	4.2	4	3.7	3.9	2.7
Bulk resistivity/ $(\Omega \cdot \text{m})$	$10^{16}$	$4 \times 10^{15}$	$7 \times 10^{14}$	$5 \times 10^{14}$	$7 \times 10^{10}$
Surface resistivity/ $\Omega$	$8 \times 10^{14}$	$5 \times 10^{14}$	$3 \times 10^{12}$	$2 \times 10^{12}$	$4 \times 10^{13}$

### 2.4 Analysis method

Each experiment consisted of eight consecutive cycles of negative half-sine voltage pulses (10 ms) followed by the 90 ms long relaxation period. The applied voltage and the PD pulse signals were recorded by the Scope Corder at the sampling rate 10 MSa/s. The acquired data includes some both the PD pulse data plus additional noise. Therefore, before further analysis, the PD signal data was digitally filtered.

The data transformed to computer were stored as '\*.WVF' format, containing the information of the relative time of each PD and the corresponding applied voltage. MATLAB codes were used to read these files to a matrix, cancel the noise, filter out each PD pulse, and plot the PD pattern. Discharge voltage (V) data was transformed to PD magnitude (pC) through PD calibrator, with the coefficient of 15.5 pC/V.

### 3. Results

Measurement results from the five different insulation plates are presented in this section. The PD pulses from the eight consecutive cycles were drawn together into a single cycle PD pattern. As the analysis was based on phase-resolved PD (PRPD) pattern, the phase of applied voltage where PD pulse occurred was substituted by the time of PD occurrence in each cycle.

As can be seen in Table 1, in addition to the pressboard, the partial discharge inception voltages (PDIV) of the other four materials are close. Test results showed that the voltages acquired for back discharge cluster to locate in each stage are also close for these four materials. In this paper, 7.6 kV, 10 kV and 13.6 kV were tested and chosen as the trigger voltages of the three stages. The PD patterns are shown in Figure 5.

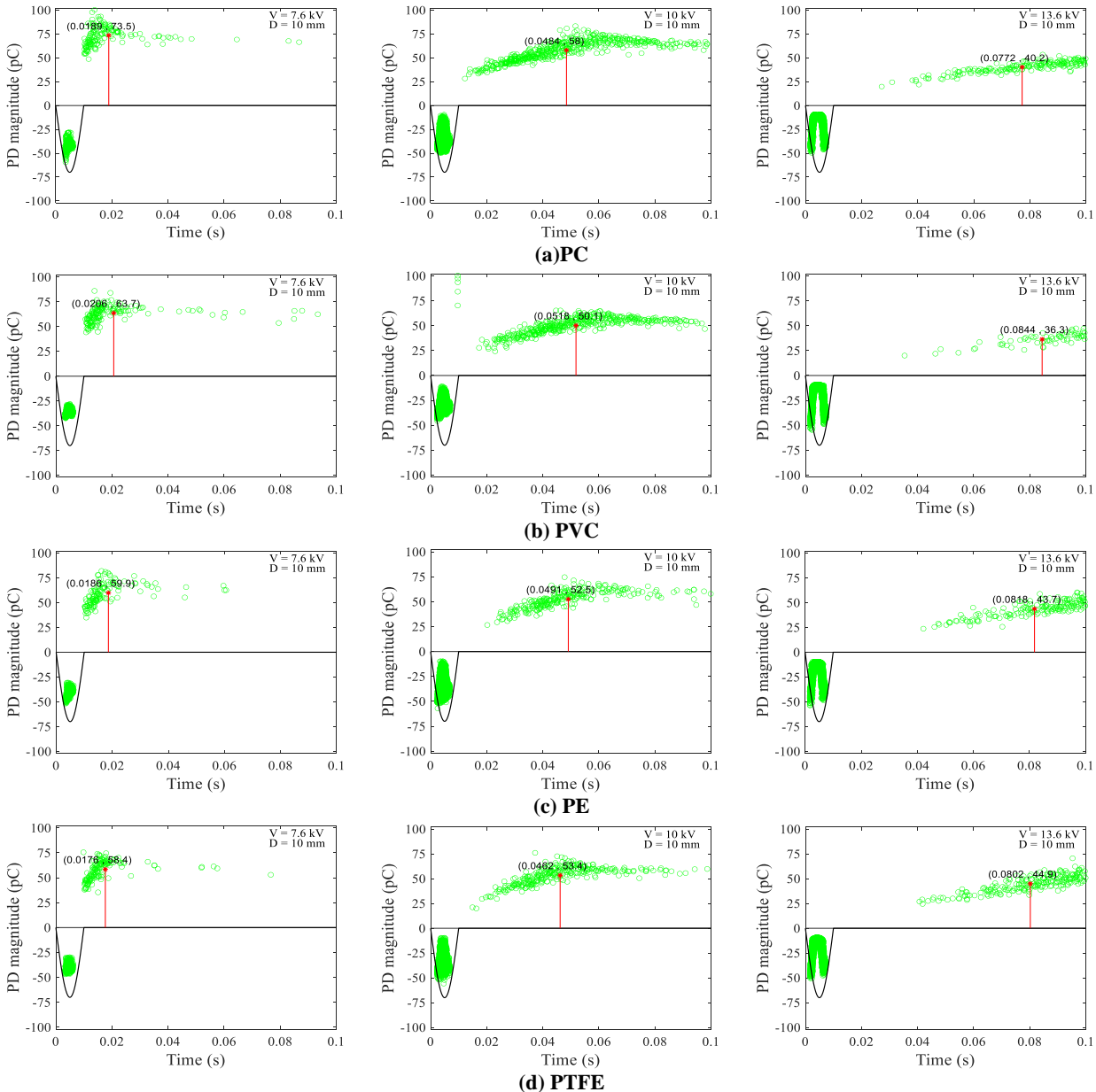


Figure 5. PD patterns of three stages for four materials: PC, PVC, PE, PTFE

Where  $V$  is the peak value of the applied voltage, and  $D$  is the air gap distance between needle tip and the insulation materials surface. The red point with stem is the feature point which indicates the average PD magnitude and PD occurrence time of all PD pulses by averaging the summation of all PD pulses during relaxation time period, as shown in Table 2.

**Table 2. Discharge information of four materials**

Material	Average PD magnitude (pC)			Average position (ms)		
	S1	S2	S3	S1	S2	S3
	PC	73.5	58	40.2	18.9	48.4
PVC	63.7	50.1	36.3	20.6	51.8	84.4
PE	59.9	52.5	43.7	18.6	49.1	81.8
PTFE	58.4	53.4	44.9	17.6	46.2	80.2

As can be found in Figure 5, the movement of back discharge cluster exists in all the four materials (PC, PVC, PE, PTFE). Some interesting regularities can be drawn:

(1) With the increase of applied voltage, the region of back discharge concentration moves forward, and with even further increased voltage, it will continue moving until it entirely ‘disappears’ in the pattern, which means there is no back discharge under repetitive unipolar voltage with relative high amplitude. This effect will be the case even if the relaxation time period is longer than in the reported experiment.

(2) With the increase of applied voltage, the average PD magnitude of back discharge cluster decreases gradually.

(3) The PD magnitude of different materials are also quite different, and there is a tendency that the PD magnitude of materials with higher resistivity are lower.

The PD pattern of pressboard under 10 kV applied voltage is shown in Figure 6.

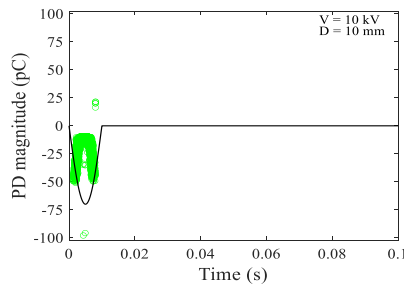


**Figure 6. PD pattern of pressboard**

Since the conductivity of the unimpregnated pressboard which would contain some moisture is much higher than that of the other four materials, the space charges more easily dissipate through pressboard and becomes injected into the ground electrode, this means that the charge accumulation ability on the surface of pressboard is far less than that of other materials, and is not able to form sufficient surface potential to generate

back discharge on the surface. This indicates that the back discharge cluster movement is caused by the space charge on the surface of insulation.

#### 4. Discussion

For needle-plane negative corona discharge model, an ionic wind happens as shown in Figure 7. As negative voltage is applied to needle electrode, an ionization region forms around the needle tip with strong electric field. Electrons are attached to oxygen molecules and the formed negative space charge will be pushed by the Coulomb force as they are sharing the same polarity with needle electrode, causing the charge transport from ionization region into drift region, following the field direction. In this movement, negative space charges collide with neutral air molecules and the momentum is transferred to the air molecules, resulting in the air molecules flowing to the surface of insulation [16]. The air flow blows away the space charges in the center of surface, forming a charge valley in the center.

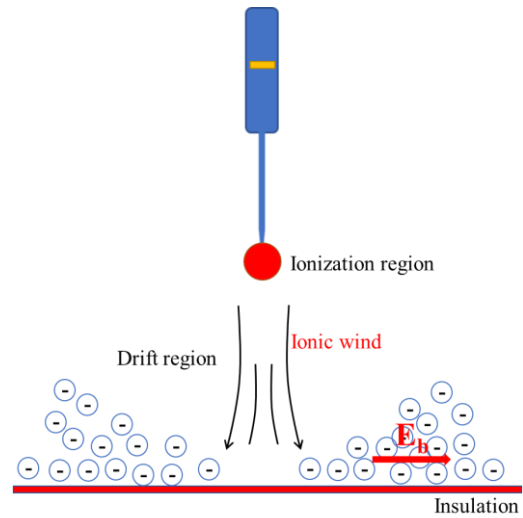


**Figure 7. Ionic wind in negative needle-plane corona discharge setup**

While turning to the relaxation time period, the potential of the needle electrode becomes 0 V, and outer charges on the surface generate a back field  $E_b$ , promoting the propagation of inner charges into the center of surface. Space charges re-accumulate in the center and finally causing the back discharge around needle tip. Higher applied voltage will generate stronger ionic wind, which will blow the charges further out, thus it takes longer time for charges to move to the center with high surface resistivity of insulation materials. This reflects in PD pattern as the movement of back discharge cluster. If further increase the applied voltage, the back discharge cluster will continue to move forward until it ‘disappears’ in the pattern. It’s because of that surface charges are too far to reposition and generate a back discharge before the coming of next cycle, and the negative voltage in next cycle will prevent the back

discharge to take place.

Due to the effect of ionic wind, the space charge density in the drift region is smaller at higher voltage instead, so the discharge magnitude decreases with the increase of applied voltage.

The material with higher resistivity turns to own lower PD magnitude at the same applied voltage. Material with higher resistivity can capture more space charges during voltage applied period, which will generate higher surface potential. Stronger back field makes it possible to produce back discharge with lower space charge density in the drift region, which causes lower PD magnitude.

## 5. Conclusion

The behavior of space charge in DBCD setup and its influence on corona discharge activity are explored. The general aim is to understand the accumulation and dissipation characteristics of space charge under unipolar voltage. The measurement method in this paper is utilizing negative half-sine voltage combined with pause time interval between each two pulses, which can simulate the space charge distribution in DC, but also generate 'PRPD' pattern. The results showed that an abnormal PD behavior could be observed through PD patterns for various insulation materials, which is that back discharges move with the variation of voltage amplitude. It was also observed that PD magnitude decreased with the increase of applied voltage. And there may be a tendency that the PD magnitude of materials with higher resistivity are lower under the same applied voltage. 'Ionic wind' theory can be an explanation on this PD anomaly and its regularities.

## Acknowledgement

The support of China Scholarship Council is gratefully acknowledged.

## References

- [1] V.V. Timatkov, G.J. Pietsch, A.B. Saveliev, et al, "Influence of solid dielectric on the impulse discharge behavior in a needle-to-plane air gap," *J. Phys. D: Appl. Phys.* vol.38, no.6, pp.877-886 2005.
- [2] A. Yehia, "Characteristics of the dielectric barrier corona discharges," *AIP Advances*, 9, 045214, pp:1-10, 2019
- [3] P. Romano, A. Imburgia, G. Rizzo, et al, "A New Approach to Partial Discharge Detection Under DC Voltage: Application to Different Materials," *IEEE Electrical Insulation Magazine*, vol.37, no.2, pp.18-32, 2021.
- [4] E. Lindell, T. Bengtsson, J. Blennow, et al, "Influence of rise time on partial discharge extinction voltage at semi-square voltage waveforms," *IEEE Transactions on Dielectrics and Electrical Insulation*, vol.17, no.1, pp.141-148, 2010.
- [5] T. Hammarström and S. M. Gubanski, "Detection of electrical tree formation in XLPE insulation through applying disturbed DC waveforms," *IEEE Transactions on Dielectrics and Electrical Insulation*, vol.28, no.5, pp.1669-1676, 2021.
- [6] T. Hammarström, "Combination of adjustable inverter level and voltage rise time for electrical stress reduction in PWM driven motor windings," *IEEE Electrical Insulation Magazine*, vol.37, no.1, pp.17-26, 2021.
- [7] K. Wu, T. Okamoto and Y. Suzuoki, "Effects of discharge area and surface conductivity on partial discharge behavior in voids under square voltages," *IEEE Transactions on Dielectrics and Electrical Insulation*, vol.14, no.2, pp.461-470, 2007.
- [8] F. Guastavino, G. Coletti, A. Ratto and E. Torello, "A study about partial discharge measurements performed applying to insulating systems square voltages with different rise times," *CEIDP '05. 2005 Annual Report Conference on Electrical Insulation and Dielectric Phenomena*, pp.418-421, 2005.
- [9] X.L. Wang, R. Clemence and H. Edin, "Partial discharge analysis of a narrow dielectric gap with repetitive half-sine pulses," *2010 Annual Report Conference on Electrical Insulation and Dielectric Phenomena*, pp.1-4, 2010.
- [10] Suwarno, Y. Suzuoki, F. Komori and T. Mizutani, "Partial discharges due to electrical treeing in polymers: phase-resolved and time-sequence observation and analysis," *J. Phys. D: Appl. Phys.*, vol.29, pp.2922-2931, 1996.
- [11] S. Suwayno and T. Mizutani, "Pulse-Sequence Analysis of Discharges in Air, Liquid and Solid Insulating Materials," *Journal of Electrical Engineering and Technology*, vol.1, no.4, pp.528-533, 2006.
- [12] S. Morsalin and B.T. Phung, "Corona discharge under non-sinusoidal voltage excitation at very low frequency," *2018 12th International Conference on the Properties and Applications of Dielectric Materials (ICPADM)*, pp.653-656, 2018.
- [13] X. Wang, N. Taylor and H. Edin, "Enhanced distinction of surface and cavity discharges by trapezoid-based arbitrary voltage waveforms," *IEEE Transactions on Dielectrics and Electrical Insulation*, vol.23, no.1, pp.435-443, 2016.
- [14] Y. Mi, L. Gui, S. Deng, et al. "Partial discharge characteristics of an air gap defect in the epoxy resin of a saturable reactor under an exponential decay pulse voltage," *IET Science, High Voltage*, vol.5, no.4, pp.482-488, 2020.
- [15] Y. Kitahara, K. Aoyagi, R. Ohyama, "An experimental analysis of ionic wind velocity characteristics in a needle-plate electrode system by means of laser-induced phosphorescence," *2007 Annual Report Conference on Electrical Insulation and Dielectric Phenomena*, pp.529-532, 2007.
- [16] F. Yin, M. Farzaneh, X. Jiang, "Simulation and laboratory investigation of ionic wind induced by corona discharge," *2016 IEEE PES Asia-Pacific Power and Energy Engineering Conference (APPEEC)*, pp.478-481, 2016.
- [17] A. Mehmood, H. Jamal, "Analysis on the propulsion of ionic wind during corona discharge in various electrode configuration with high voltage sources," *2019 International Conference on Applied and Engineering Mathematics (ICAEM)*, pp.7-12, 2019.
- [18] K. Shimizu, Y. Mizuno, M. Blajan, "Basic study on flow control by using plasma actuator," *IEEE Transactions on Industry Applications*, vol.51, no.4, pp.3472-3478, 2015.